

FOXF2 Regulates PRUNE2 Transcription in the Pathogenesis of Colorectal Cancer

Ting Li, MM^{1,2,3,4}, Silin Huang, MM^{4,5}, Wei Yan, MM^{1,6},
Yu Zhang, MD^{2,3}, and Qiang Guo, MD^{2,3} 

Technology in Cancer Research & Treatment
Volume 21: 1-12
© The Author(s) 2022
Article reuse guidelines:
sagepub.com/journals-permissions
DOI: 10.1177/15330338221118717
journals.sagepub.com/home/tct



Abstract

Background: Forkhead box F2, a member of the Forkhead box transcription factor superfamily, plays an important role in several types of cancer. However, the mechanisms of Forkhead box F2 in the progression of colorectal cancer remain unclear. PRUNE2 is closely associated with prostate cancer, neuroblastoma, glioblastoma, and melanoma. The relationship between Forkhead box F2 and PRUNE2 in colorectal cancer remains unknown. **Method:** We investigated the effects of Forkhead box F2 upregulation on colorectal cancer cell behavior *in vitro* using Cell Counting Kit-8, colony formation, flow cytometry, Transwell, reverse transcription quantitative polymerase chain reaction and Western blot analyses. Nude mouse xenografts were established to investigate the effect of Forkhead box F2 upregulation on the growth of colorectal cancer cells. Dual-luciferase reporter assays were performed to confirm the Forkhead box F2 regulation of PRUNE2 transcription. A series of *in vitro* assays was performed in cells with Forkhead box F2 upregulation and PRUNE2 knockdown to elucidate the function and regulatory effects of Forkhead box F2 on PRUNE2 transcription in colorectal cancer. **Results:** Forkhead box F2 was downregulated in colorectal cancer tissues compared with adjacent tissues. Forkhead box F2 overexpression significantly suppressed the proliferation and invasion of colorectal cancer cells *in vitro* and *in vivo*. Moreover, Forkhead box F2 directly targeted PRUNE2 to promote its transcription in colorectal cancer cells. Furthermore, PRUNE2 mediated the Forkhead box F2-regulated proliferation and invasion of colorectal cancer cells. Additionally, we demonstrated a significant positive correlation between Forkhead box F2 and PRUNE2 mRNA levels in colorectal cancer tissues. **Conclusion:** These results indicated that Forkhead box F2 and PRUNE2 in combination may serve as a prognostic biomarker for colorectal cancer and that Forkhead box F2 upregulation inhibits the proliferation and invasion of colorectal cancer cells by upregulating PRUNE2.

Keywords

colorectal cancer, FOXF2, PRUNE2, regulation, pathogenesis

Abbreviation

FOX, Forkhead box; CRC, colorectal cancer; CCK-8, Cell Counting Kit-8; qPCR, quantitative polymerase chain reaction; IARC, International Agency for Research on Cancer; WHO, World Health Organization; HCC, hepatocellular carcinoma; CRC, colorectal cancer; PC, prostate cancer; GC, gastric cancer; OC, ovarian cancer; TCGA, The Cancer Genome Atlas; IHC, immunohistochemistry; PBS, phosphate-buffered saline; FBS, fetal bovine serum; siRNA, small interfering RNA; TSS, transcription start site; SDS-PAGE, sodium dodecyl sulfate-polyacrylamide gel electrophoresis; PVDF, polyvinylidene difluoride; PI, propidium iodide; SD, standard deviation

Received: February 10, 2022; Revised: July 18, 2022; Accepted: July 22, 2022.

¹ Faculty of Environmental Science and Engineering, Kunming University of Science and Technology, Kunming, Yunnan, China

² Department of Gastroenterology, The First People's Hospital of Yunnan Province, Kunming, Yunnan, China

³ Department of Gastroenterology, The Affiliated Hospital of Kunming University of Science and Technology, China

⁴ Medical School, Kunming University of Science and Technology, Kunming, Yunnan, China

⁵ Department of Gastroenterology, South China Hospital, Health Science Center, Shenzhen University, Shenzhen, China

⁶ Faculty of Life Science and Technology, Kunming University of Science and Technology, Kunming, Yunnan, China

Corresponding Author:

Qiang Guo, MD, Department of Gastroenterology, The First People's Hospital of Yunnan Province, Kunming 650032, Yunnan, China.

Email: gqkj003@sina.com Yu Zhang, MD, Department of Gastroenterology, The First People's Hospital of Yunnan Province, Kunming 650032, Yunnan, China.

Email: yuzhang320@sina.com



Creative Commons Non Commercial CC BY-NC: This article is distributed under the terms of the Creative Commons Attribution-NonCommercial 4.0 License (<https://creativecommons.org/licenses/by-nc/4.0/>) which permits non-commercial use, reproduction and distribution of the work without further permission provided the original work is attributed as specified on the SAGE and Open Access page (<https://us.sagepub.com/en-us/nam/open-access-at-sage>).

Introduction

According to global cancer statistics from the International Agency for Research on Cancer (IARC), which is part of the World Health Organization (WHO), approximately 1.85 million new cases of colon, rectal, and anal malignancies (“colorectal cancer”, or CRC, for short) were diagnosed in 2018 worldwide, ranking third on the spectrum of malignant tumors. The mortality of CRC ranks second among all malignant tumors, as it is estimated to have caused 880 000 deaths.¹ Over the past 10 years, the incidence and mortality of CRC have continually increased in China, thus causing a prominent problem that endangers the health of the population.² The prognosis of patients with CRC is not ideal, and new treatment regimens are urgently needed. Molecular targeted therapies have become a new trend in CRC due to their advantages of high efficiency and low toxicity. Therefore, elucidation of the molecular mechanisms underlying the occurrence and development of CRC and identification of new biomarkers for new targeted therapies are expected to benefit patients who are ineligible for radical surgery.

The forkhead box (FOX) transcription factor family was first discovered in fruit flies³ and is now divided into 19 subfamilies, namely, FOXA-FOXS.⁴ The most distinctive feature of their structure is the FOX DNA-binding domain, which is composed of more than 100 conserved amino acid sequences.⁵ The FOX gene family mediates a variety of biological functions, such as DNA damage repair, embryonic development, the cell cycle, and some metabolic balance regulation,^{6,7} suggesting its involvement in the complex processes of tumorigenesis. Forkhead box transcription factor F2 (FOXF2) protein, a member of the FOX transcription factor family, contains 444 amino acid residues and is located on chromosome 6p25.3 in humans. FOXF2 is mainly expressed in the epithelial–mesenchymal cells of the respiratory tract, digestive tract, urinary tract, and other organs and is involved in extracellular matrix synthesis, mutual transformation between the epithelium and mesenchymal tract, and embryonic and tissue development.^{8–10} FOXF2 is correlated with tumor progression, metastasis of breast cancer,^{11,12} lung cancer,^{13–15} hepatocellular carcinoma (HCC),^{16,17} colorectal cancer (CRC),^{18–22} prostate cancer (PC),^{23–25} gastric cancer (GC),^{26,27} oral cancer,²⁸ ovarian cancer (OC),²⁹ mouse rhabdomyosarcoma,³⁰ bladder cancer,³¹ and esophageal squamous cell carcinoma.³² FOXF2 has shown inhibitory effects in most tumors, such as liver cancer^{16,17} and prostate cancer,²⁵ and shown tumor-promoting effects in lung cancer¹⁴ and mouse rhabdomyosarcoma.³⁰ However, FOXF2 plays either an inhibitory or promotional role in breast cancer.^{11,12,33,34} FOXF2 was downregulated in 76.0% of CRC samples and could be a potential diagnostic biomarker in CRC.¹⁸ However, the mechanism underlying the effect of FOXF2 on CRC development is still unclear.

PRUNE2 (prune homolog 2, *Drosophila*) encodes a 340-kDa protein that has a conserved BNIP-2 and Cdc42GAP homology (BCH) scaffold domain at its C-terminus.³⁵ PRUNE2 is a specific prognostic gene in neuroblastoma and

plays an important role in regulating the differentiation, proliferation, and invasion of neuroblastoma cells.³⁶ PRUNE2 plays an important role in regulating the growth of tumors, such as leiomyosarcoma,³⁷ oral cancer,³⁸ prostate cancer,^{39,40} and neuroblastoma.⁴¹ Our previous study found that the expression of PRUNE2 was significantly reduced in CRC patients, and the survival prognosis of patients with low expression of PRUNE2 was poor. Overexpression of PRUNE2 significantly inhibited the proliferation, migration, and invasion of CRC cells and significantly inhibited the growth of CRC cells in nude mice, suggesting that PRUNE2 inhibits the growth of CRC *in vivo* and *in vitro*.⁴² However, the association between FOXF2 and PRUNE2 expression in CRC is poorly understood.

In this study, we investigated the expression of FOXF2 in CRC using human CRC tissue samples and cell lines and then assessed the effect of FOXF2 upregulation on CRC *in vitro* and *in vivo*. Furthermore, for the first time, we investigated the transcriptional regulatory relationship between FOXF2 and PRUNE2 in CRC cells and the underlying regulatory mechanism. Our data indicated that FOXF2 upregulation inhibited the proliferation and invasion of CRC *in vivo* and *in vitro*. FOXF2 was shown to bind the promoter region of PRUNE2 and regulate its transcription, thereby affecting the pathogenesis of CRC.

Materials and Methods

Gene Expression Analyses and Tissue Specimens Collection

FOXF2 mRNA expression levels were analyzed using data from The Cancer Genome Atlas (TCGA).⁴³ In total, 35 CRC tissue specimens and 11 adjacent tissue sections were collected from the Department of Gastroenterology at the First People’s Hospital of Yunnan Province for quantitative polymerase chain reaction (qPCR), immunohistochemistry (IHC) and Western blot analyses. This study was approved by the Medical Ethics Committee of the First People’s Hospital of Yunnan Province (no. KHLL2021-KY130), and written consent was obtained from all participants.

Immunohistochemistry

Tissues were routinely paraffin-embedded, sliced into 4- μ m-thick sections, and then subjected to xylene dewaxing and gradient alcohol (100%, 95%, 90%, 80%, and 70% ethanol) rehydration. The slides were washed 3 times with phosphate-buffered saline (PBS; P1020; Solarbio), boiled in sodium citrate antigen retrieval solution (C1031; Solarbio, Beijing, China) at 95 °C to 100 °C in a pressure cooker for 10 min, and then immersed in 3% hydrogen peroxide for 15 min to block endogenous peroxidase. Then, the slides were blocked with 5% goat serum (SL038; Solarbio) for 15 min at room temperature. Subsequently, the slides were incubated with primary antibodies against FOXF2 (1:1000; CSB-PA027320; CUSABIO) and PRUNE2 (1:100; 11458-1-AP;

ProteinTech) at 4 °C overnight. The slides were washed 3 times with PBS and then incubated with an HRP goat antirabbit IgG secondary antibody (1:200; cat. no. AS014; ABclonal) for 1 h at room temperature. They were then stained with 3,3-diaminobenzidine (DAB, DA1015; Solarbio), counterstained with hematoxylin (G1140; Solarbio) for 5 min at room temperature and mounted with neutral gum after dehydration.⁴⁴ All slides were observed by a blinded investigator under a light microscope. Brown staining indicated immunoreactive (positive) cells; blue staining indicated nuclei. Positive expression was quantified using ImageJ 2× software (National Institutes of Health).

Cell Culture

Human CRC cell lines [SW620 (CCL-227), SW480 (CCL-228), HT29 (HTB-38), HCT116 (CCL-247), LOVO (CCL-229), DLD-1 (CCL-221)] and normal colorectal mucosa cells (FHC; CRL-1831) were obtained from the Chinese Academy of Sciences Cell Bank (Shanghai, China). All cells were maintained in high-glucose Dulbecco's Modified Eagle's medium (DMEM, C11995500BT; Gibco) supplemented with 10% fetal bovine serum (FBS; 10270-106; Gibco) and antibiotics (03-031-1B; Biological Industries). All cells were cultured in a humidified incubator at 37 °C with 5% CO₂.

Plasmids, Small Interfering RNA, and Transfection

The full-length coding region of FOXF2 cDNA was amplified by PCR from normal human cells, inserted into the mammalian expression vector pcDNA3.1, and then confirmed by sequencing. A small interfering RNA (siRNA) targeting human PRUNE2 (siPRUNE2; GGGCCAGAATATCGATGAATT) and a nontargeting siRNA control (siControl; UUCUCCGAACGUGUCAC GUTT) were synthesized by GenePharma Company. Transient transfection of the plasmids or siRNAs into cells was performed using Lipofectamine 2000 (11668-019; Invitrogen) according to the manufacturer's protocol. For cell transfection, 1×10^5 cells were plated in a 6-well plate at 37 °C overnight. Then, 100 pmol of siPRUNE2 or NC siRNA or 2 µg of pcDNA3.1-FOXF2 or empty pcDNA3.1 vector and 15 µL of Lipofectamine were incubated at room temperature for 20 min. The mixtures were transfected into cells for 48 h. The efficiency of transfection was determined by Western blot.

Dual-Luciferase Reporter Assay

To detect the potential sites at which FOXF2 may bind to the promoter region of PRUNE2, the luciferase reporter vector pGL3-basic (Promega) was used to construct PRUNE2 promoter reporters (pPRUNE2 #1, pPRUNE2 #2, pPRUNE2 #3, and pPRUNE2 #4). PRUNE2 promoter regions (from -2000 to 151, -1800 to 151, -1649 to 151, and -1000 to 151) in relation to the transcription start site (TSS) were synthesized by GenePharma. The PCR products were then inserted into the pGL3-basic vector. HT29 cells were plated in 12-well plates

at a density of 5×10^4 cells/well and cultured without antibiotics for 24 h. The cells were then cotransfected with pGL3-PRUNE2 and pcDNA3.1-FOXF2 as well as with the pcDNA3.1 vector as mentioned above. After 48 h, the luciferase activity was measured using the Dual-Luciferase Reporter Assay System (E1910; Promega). Luciferase activity was normalized to that of Renilla, and the experiments were performed in triplicate.

Quantitative Real-Time PCR Assay

Total RNA was extracted using TRIzol (1596-026; Invitrogen) according to the manufacturer's instructions. A RevertAid First Strand cDNA Synthesis Kit (K1622; Fermentas) was used to reverse transcribe the RNA into cDNA in accordance with the manufacturer's protocol, and qPCR was performed by using THERMO Maxima SYBR Green/ROX qPCR Master Mix (K0223; Thermo) according to the manufacturer's instructions as follows: 95 °C for 3 min; followed by 40 cycles of 95 °C for 10 s and 60 °C for 60 s. All samples were normalized to β-actin, and all experiments were performed in triplicate. The mean value of each triplicate was used to calculate the relative mRNA expression levels using the $2^{-\Delta\Delta CT}$ method.⁴⁵ The following primer sequences were synthesized by Sangon Biotech as follows: FOXF2-forward: 5'-TACCAGCATCACTCTACTC-3', FOXF2-reverse: 5'-ATCCGTCGCCAGTTTCTATC-3'; PRUNE2-forward: 5'-GGGTCTTCTGGGATTATGG-3', PRUNE2-reverse: 5'-CTGGGCTAACAAGGTCTAC-3', and β-actin-forward: 5'-CATCGTCCACCGCAAATGCTTC-3', β-actin-reverse: 5'-AACCGACTGCTGTACCTTCAC-3'.

Western Blot Assay

Total proteins were extracted from tissues and cells with RIPA lysis buffer (R0020; Solarbio), and then quantified by a BCA Protein Assay Kit (PC0020; Solarbio) according to the manufacturer's protocol. A total of 30 µg of protein per lane was separated by 10% sodium dodecyl sulfate-polyacrylamide gel electrophoresis (SDS-PAGE) for 120 min at 120 V before being transferred onto polyvinylidene difluoride (PVDF) membranes (IPVH00010; Millipore). Subsequently, the membranes were blocked with 5% skim milk for 2 h at room temperature and then incubated with a specific primary antibody targeting FOXF2 (1:1000; CSB-PA027320; CUSABIO), PRUNE2 (1:1000; 11458-1-AP; ProteinTech), or β-actin (1:2000; ab8227; Abcam) overnight at 4 °C. The membranes were then incubated with HRP-conjugated goat antirabbit antibodies (1:2000; A0208, Beyotime), and β-actin was used as the loading control. The bands were developed using a ChemiDoc XRS⁺ Imaging System (Bio-Rad) and Immobilon Western Chemiluminescent HRP Substrate (WBKLS0100; Millipore Fontenay-Sous-Bois). The band densities of specific proteins were quantified using ImageJ 2× software (National Institutes of Health).

CCK-8 Assay

Briefly, 10000 cells were seeded into each well of a 96-well plate. After incubation at 37 °C for 24 h, the cells were transfected with pcDNA3.1-FOXF2 or/and PRUNE2 siRNA for 48 h, 10 µL of CCK-8 solution (CP002; SAB) was added to each well, and the cells were incubated at 37 °C for 2 h. The absorbance was measured at 450 nm using a microplate reader (DNM-9602; PERLONG).

Colony Formation Assay

Cells were plated in a 10-mm culture dish at a density of 700 cells/well and cultured at 37 °C for 24 h in an incubator. The next day, the cells were transfected with pcDNA3.1-FOXF2 or/and PRUNE2 siRNA for 48 h and further cultured for 7 days. The medium was replaced with fresh medium every 3 days. Finally, the cells were washed with PBS 3 times and stained with 0.5% crystal violet (C8470; Solarbio) for 15 min at room temperature; colonies with more than 50 cells were counted in the entire well.

Cell Invasion Assay

Cell invasion *in vitro* was assessed using Matrigel-coated 8-µm Transwell (BD Biosciences). Briefly, 200 µL of cells (4×10^5 cells/mL) was added to the upper Transwell chamber, and 700 µL of complete medium was added to the lower Transwell chamber. After transfection for 48 h, the cells were fixed with 4% formaldehyde for 10 min at room temperature, and the invaded cells were then stained with 0.5% crystal violet (C8470; Solarbio) for 30 min at room temperature. The number of invading cells on the lower membrane surface was counted under a microscope in 5 predetermined fields for each membrane at 200× magnification.

Cell Cycle Assay

After transfection for 48 h, 1×10^5 cells were harvested and resuspended in 1 mL of 70% ethanol overnight at 4 °C. Then, the cells were incubated in 100 µL of RNase A solution (1 mg/mL; R8020-25; Solarbio) in the dark at 37 °C for 30 min and then with 400 µL of propidium iodide (PI) solution (50 µg/mL; C001-200; 7Sea Biotech) in the dark at room temperature for 10 min. The cell cycle was detected on a flow cytometer (Accuri C6) according to the manufacturer's instructions. BD Accuri C6 plus software (3.1.1.0; BD Biosciences) was used for analysis. Red fluorescence was detected at an excitation wavelength of 488 nm, corresponding to the BD Biosciences flow cytometry FL2 detection channel.

Cell Apoptosis Assay

Cell apoptosis was detected using an annexin V-APC/PI dual staining kit (E-CK-A151; Elabscience). After transfection for 48 h, 1×10^5 cells were harvested and resuspended in 195 µL of annexin V-APC binding buffer. Then, 5 µL of annexin

V-APC staining solution was added to the cells in the dark at 4 °C for 15 min, followed by the addition of 5 µL of PI staining solution in the dark at 4 °C for 5 min. Apoptosis was detected on a flow cytometer (Accuri C6) according to the manufacturer's instructions. BD Accuri C6 plus software (3.1.1.0; BD Biosciences) was used for analysis. The percentage of apoptotic cells was calculated as the sum of the percentage of early apoptotic cells and late apoptotic cells.

Xenograft Tumor Assay

Twelve female BALB/c nude mice (weight, 18 ± 2 g; age, 6-8 weeks; Charles River Laboratories, Inc.) were reared in a sterile environment at 21 °C to 25 °C with 40% to 70% humidity and a 12/12-h light/dark cycle for one week. The animal study was approved by the Ethics Committee of Shanghai Genechem Co., Ltd (no. GSZE0260446) on December 15, 2020, and performed in compliance with Chinese national guidelines for the care and use of animals. HT29 cells were infected with the pGV492 vector lentivirus (KL2117-2; Genechem) and FOXF2 overexpression lentivirus (44482-2; Genechem). After 48 h of infection, the cells were trypsinized with 0.25% trypsin (25200056; Gibco, California, USA) and subcultured. Following cell adherence, puromycin (cat. no. P8230; Beijing Solarbio Science & Technology Co., Ltd) was added at 5 µg/mL to screen the cells, and the solution was replaced with complete DMEM supplemented medium with 5 µg/mL puromycin every 2 to 3 days. After 1 week, the cells were cultured in complete medium containing 2 µg/mL puromycin. qPCR was performed to verify the expression levels of FOXF2 in the screened FOXF2 overexpressing HT29 and vector-HT29 cells (data not shown). The successfully screened cell lines were named FOXF2 and Vector. In total 1×10^7 vector or FOXF2 cells in 0.1 mL of PBS were subcutaneously injected into the dorsal side of the right hind limb. The mice were randomly divided into 2 groups for the xenograft tumor assay: the Vector group and the FOXF2 group ($n = 6$ /per group). After 13 days, all mice were anesthetized with pentobarbital sodium (50 mg/kg) by intraperitoneal injection, and the fluorescence at the cell inoculation sites was then observed using an IVIS Spectrum *In Vivo* Bioluminescence imaging system (Lumina LT; PerkinElmer). The living image data are expressed as the total radiant efficiency [p/s]/[µW/cm²]. A Vernier caliper was used to measure the long (L) and short (W) diameters of subcutaneous tumors at 6, 8, 10, 12, and 13 days after injection. Tumor volume was calculated according to the following formula: $3.14/6 \times L \times W^2$. At 13 days, all nude mice were euthanized by an intraperitoneal injection of pentobarbital sodium (150 mg/kg) followed by cervical dislocation to remove the subcutaneous tumors. The tissues were paraffin-embedded, sectioned, and subjected to IHC staining.

Statistical Analysis

Data are presented as the mean \pm standard deviation (SD). All experiments were conducted in triplicate, and all results were

analyzed using GraphPad Prism 5.0 software (GraphPad Software, Inc). Differences between 2 groups were analyzed by unpaired Student *t* test, while those among multiple groups were compared by one-way ANOVA (post hoc test). Pearson's correlation coefficient was used to determine the correlation between FOXF2 and PRUNE2 mRNA expression in CRC tissues. $P < .05$ was considered to be significant.

Results

FOXF2 Expression Is Decreased in CRC Tissues

Statistical analysis of mRNA expression data from TCGA showed that FOXF2 was expressed at low levels in CRC compared to normal tissues (Figure 1A; $P < .05$). IHC analysis also revealed significantly fewer FOXF2-positive cells in CRC tissues than in adjacent tissues (Figure 1B; $P < .001$). In addition, the FOXF2 protein levels were significantly decreased in CRC tissues compared with adjacent tissues (Figure 1C; $P < .001$). Furthermore, FOXF2 expression was also assessed in

human normal colorectal mucosa cells (FHC) and 6 CRC cell lines (SW620, SW480, HT29, HCT116, LOVO, DLD-1) by Western blot. As shown in Figure 1D, consistent with the results obtained with the tissue samples, FOXF2 expression was significantly decreased ($P < .001$) in the 6 CRC cell lines.

FOXF2 Overexpression Inhibits CRC Cell Proliferation and Invasion and Induces Apoptosis in Vitro

To investigate the effects of FOXF2 on CRC cell proliferation, invasion, and apoptosis, pcDNA3.1-FOXF2 was transfected into SW620 and HT29 cells to upregulate FOXF2 expression. The effects of pcDNA3.1-FOXF2 transfection on FOXF2 expression were confirmed by Western blot. The FOXF2 protein levels in both SW620 and HT29 cells transfected with pcDNA3.1-FOXF2 were obviously reduced ($P < .01$ and $P < .05$, respectively) compared with those in the vector-transfected cells (Figure 2A). The Cell Counting Kit-8 (CCK-8) results revealed that FOXF2 overexpression suppressed the

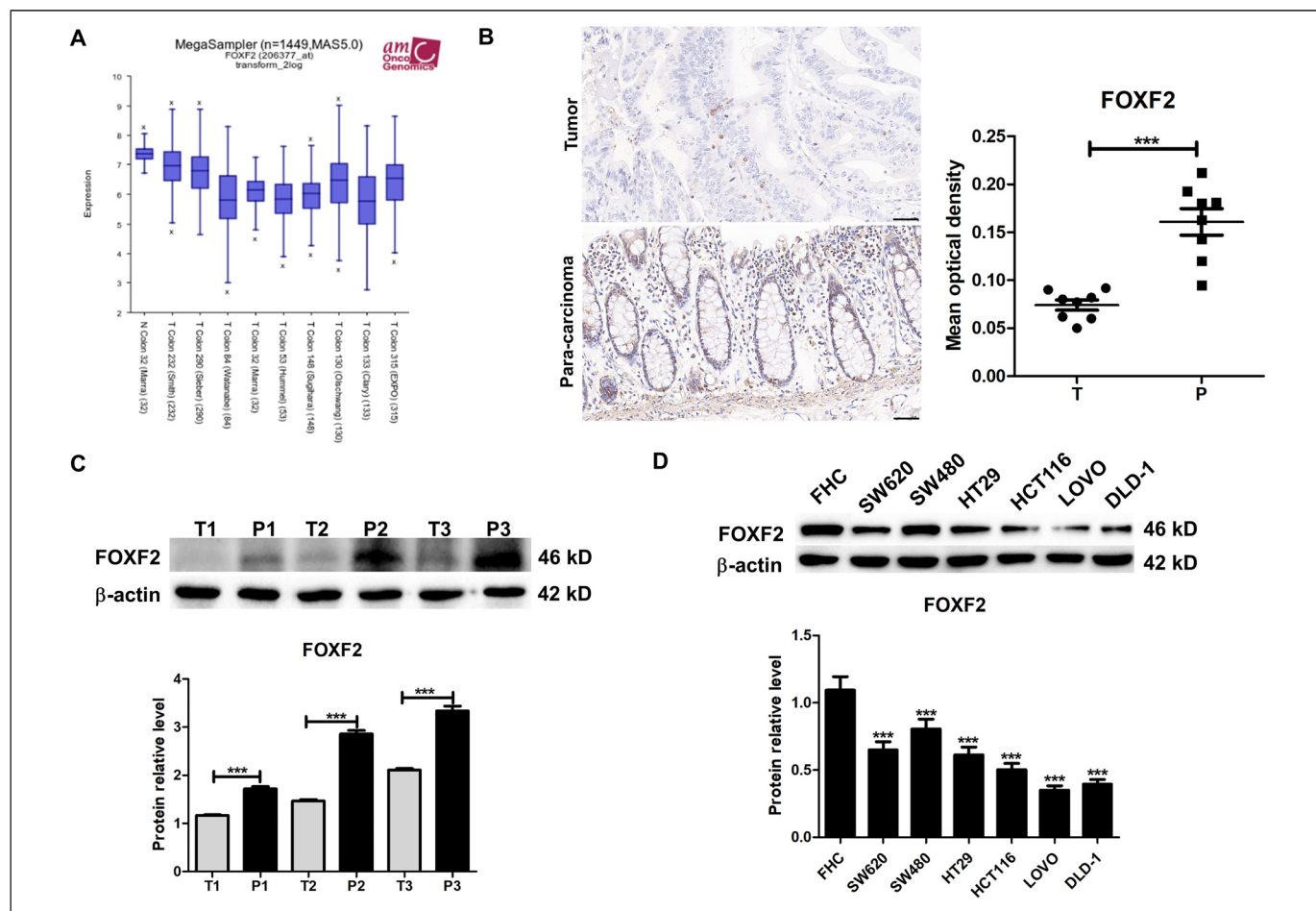


Figure 1. FOXF2 expression in CRC tissues and cell lines. (A) The expression levels of FOXF2 were analyzed in CRC tissues and normal tissues from the TCGA database. (B) FOXF2 expression in tumorous ($n = 8$) and peritumorous tissues ($n = 8$) was analyzed by IHC (magnification at 400 \times , left). Scale bar = 50 μ m. Quantification of FOXF2 expression using ImageJ software (right). (C) Western blot analysis was performed to detect FOXF2 expression in tumor ($n = 3$) and peritumorous tissues ($n = 3$). (D) FOXF2 expression in different cell lines was analyzed by Western blot. Three independent assays were performed in triplicate. The data are expressed as the mean \pm SD. *** $P < .001$.

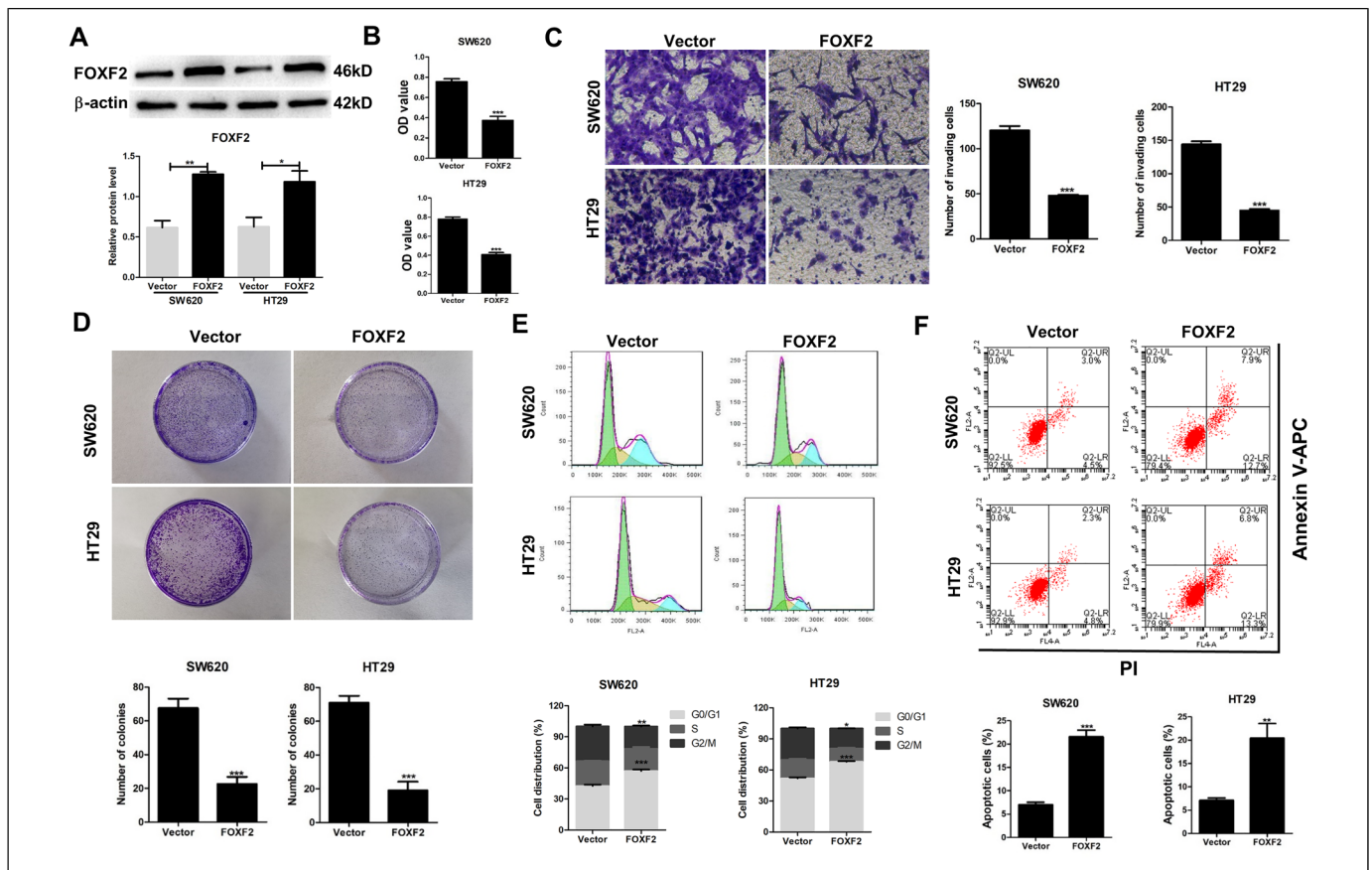


Figure 2. FOXF2 overexpression suppresses CRC cell proliferation, invasion, and apoptosis *in vitro*. (A) Western blot was performed to verify the overexpression of FOXF2 in SW620 and HT29 cells transfected with pcDNA3.1-FOXF2. (B) The viability of CRC cells was detected by the Cell Counting Kit-8 (CCK-8) assay. (C) Representative images of the Transwell assay are shown. Magnification, 200 \times . The number of invaded cells was counted. (D) Colony formation of CRC cells as determined by staining with crystal violet. The number of stained colonies in CRC cells was counted. (E) Flow cytometry analysis of cell cycle progression. The quantified results of the cell cycle distribution are shown. (F) The apoptosis of CRC cells was detected by flow cytometry with an annexin V-APC/PI double staining kit. The apoptotic cell percentages are shown in the top right and bottom right quadrants. Three independent assays were performed in triplicate. The data are expressed as the mean \pm SD. * P < .05; ** P < .01; *** P < .001.

proliferation of the 2 cell lines (Figure 2B; P < .001). Transwell assays showed that FOXF2 overexpression significantly inhibited the invasion of the 2 cell lines (Figure 2C; P < .001). Furthermore, FOXF2 overexpression significantly decreased the number of cell colonies (Figure 2D; P < .001). Flow cytometry analysis showed that the upregulation of FOXF2 arrested CRC cells at the G0/G1 stage (Figure 2E; P < .001) and induced apoptosis in the 2 cell lines (Figure 2F; P < .001 and P < .01, respectively).

FOXF2 Binds to the PRUNE2 Promoter and Promotes Its Transcription

The role of FOXF2 in CRC progression was consistent with that of PRUNE2 revealed in our previous study. To investigate whether PRUNE2 is a transcriptional target of FOXF2, we analyzed the FOXF2 binding sites in the promoter region of the PRUNE2 gene using an online tool (<http://jaspar2016>.

genereg.net/). Seventeen putative FOXF2 binding sites were identified in the FOXF2 promoter region at -2000 to $+151$, -1800 to $+151$, -1649 to $+151$, and -1000 to $+151$ bp (Figure 3A). Subsequently, we constructed 4 PRUNE2 promoter luciferase reporter constructs (pPRUNE2 #1-4) containing sequential deletions of the candidate FOXF2 binding sites, as shown in Figure 3B, and then performed a dual-luciferase reporter assay in HT29 cells cotransfected with pGL3-PRUNE2 and pcDNA3.1-FOXF2 or the pcDNA3.1 vector. The relative luciferase activity of pPRUNE2 #2, containing the S7-S14 binding sites in HT29 cells, was higher than those of pPRUNE2 #1 and other vectors lacking these sites. The overexpression of FOXF2 significantly enhanced the relative luciferase activity of pPRUNE2 #2, containing S7-S14 binding sites, compared with that in the vector group (Figure 3B; P < .001), suggesting that FOXF2 mainly activates the PRUNE2 promoter by directly binding to the S7 to S14 regions. Furthermore, the ability of FOXF2 to positively regulate PRUNE2 protein expression was confirmed by the

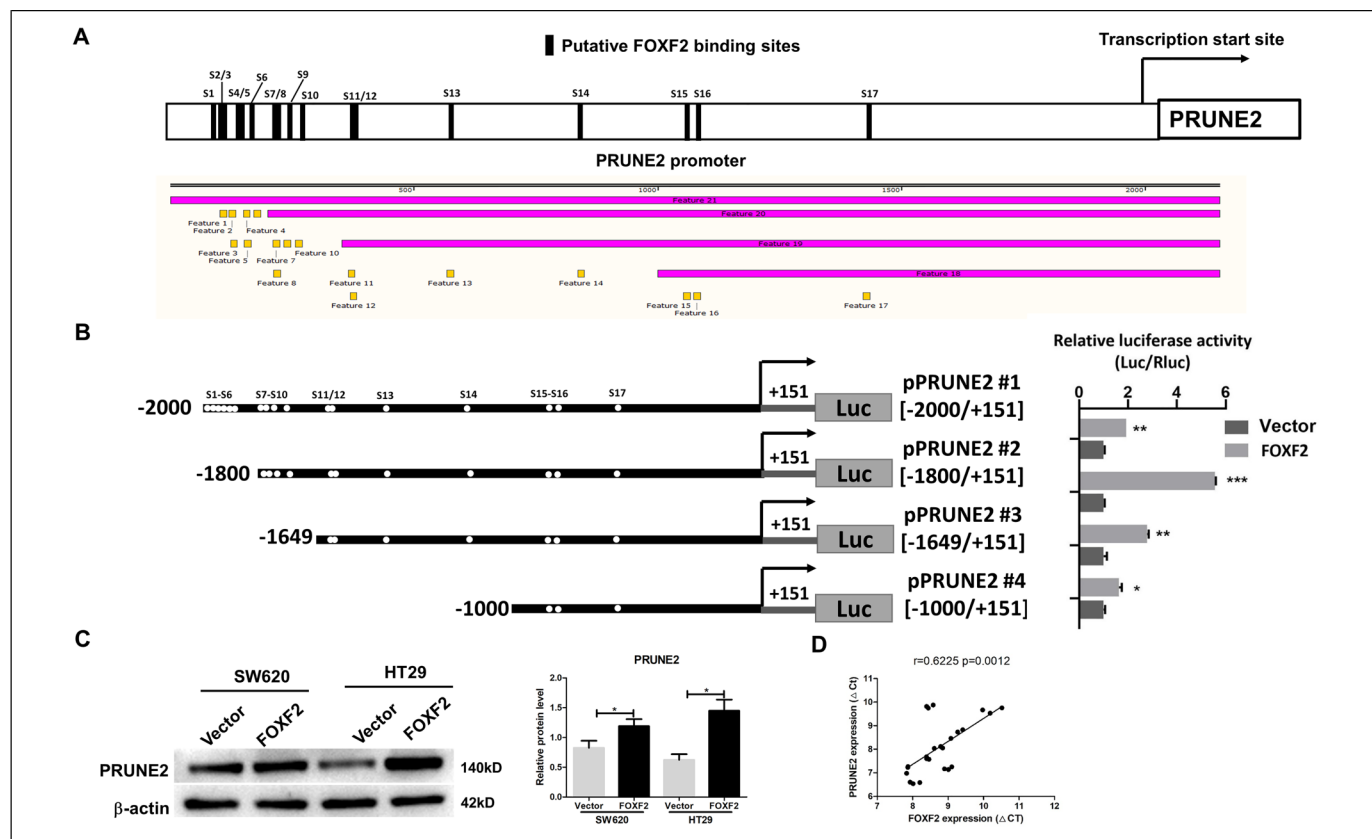


Figure 3. FOXF2 positively regulates PRUNE2 expression by targeting and activating the FOXF2 promoter. (A) Schematic of the putative binding sites of FOXF2 on the PRUNE2 promoter region. (B) The transcriptional activity of the PRUNE2 promoter in HT29 cells was assessed by the dual-luciferase reporter assay. (C) The protein levels of PRUNE2 in the 2 cell lines were detected by Western blot. (D) FOXF2 and PRUNE2 mRNA levels were positively correlated in human CRC tissues ($n = 24$; Pearson's correlation $r = 0.6225$, $P = .0012$). Three independent assays were performed in triplicate. The data are expressed as the mean \pm SD. * $P < .05$; ** $P < .01$; *** $P < .001$.

overexpression of FOXF2 in SW620 and HT29 cells, as determined by Western blot (Figure 3C). Furthermore, we also detected the mRNA levels of FOXF2 and PRUNE2 in 24 human CRC tissues by qPCR. Consistent with the positive regulatory effects of FOXF2 on the transcription of PRUNE2, the PRUNE2 mRNA levels were similarly correlated with those of FOXF2 in CRC (Pearson's $r = 0.6225$, $P = .0012$; Figure 3D).

PRUNE2 Mediates the FOXF2-Regulated Suppression of CRC Aggressiveness

To further investigate whether PRUNE2 mediates the ability of FOXF2 deficiency to induce the proliferation and invasion of CRC cells, SW620 and HT29 cells were cotransfected with pcDNA3.1-FOXF2 (FOXF2) and PRUNE2 siRNAs (siPRUNE2) or their controls and then subjected to CCK-8, colony formation, Transwell, and flow cytometry assays. As shown in Figure 4, downregulation of PRUNE2 partially reversed the FOXF2 overexpression-induced inhibition of cell proliferation (Figure 4A; $P < .01$ and $P < .001$, respectively), invasion (Figure 4B; both $P < .001$), and cell colony numbers (Figure 4C; $P < .001$ and $P < .01$, respectively). Flow cytometry

analysis showed that downregulation of PRUNE2 promoted cell cycle progression, which was arrested by FOXF2 overexpression (Figure 4D). In addition, downregulation of PRUNE2 inhibited the increase in cell apoptosis induced by FOXF2 overexpression (Figure 4E; $P < .001$ and $P < .01$, respectively).

FOXF2 Overexpression Suppresses the Aggressiveness of CRC in BALB/c Mice *in Vivo*

To further confirm the effects of FOXF2 on the growth of CRC cells *in vivo*, HT29 cells infected with a negative control lentivirus or LV-GFP-FOXF2 were injected into the dorsal sides of the right hind limbs of female nude mice. Visible tumor nodules were observed in the mice of the 2 groups (Figure 5A), and the tumors of mice injected with LV-GFP-FOXF2 cells (FOXF2 group) were smaller than those of mice injected with the negative control lentivirus cells (Vector group) by day 13 after injection. The tumors in the FOXF2 group weighed less than those in the Vector group ($P < .001$), while the volumes of xenograft tumors in mice of the FOXF2 group were smaller than those of mice from the Vector group (Figure 5B; $P < .001$). On day

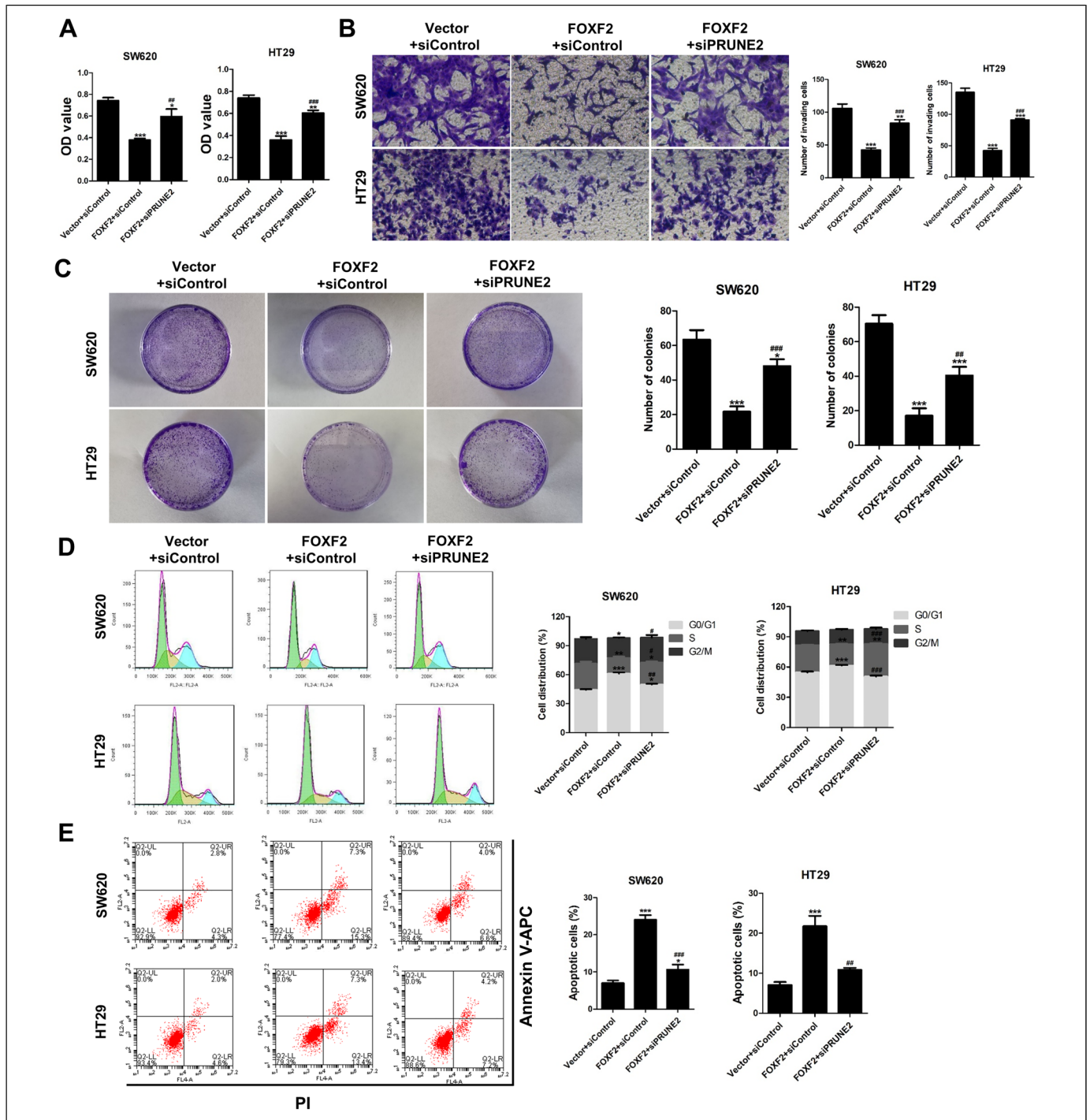


Figure 4. FOXF2 overexpression inhibits CRC proliferation and invasion by upregulating PRUNE2 transcription. (A) The proliferation of SW620 and HT29 cells was detected by Cell Counting Kit-8 (CCK-8) assays. (B) Images and numbers of invaded SW620 and HT29 cells as determined by the Transwell assay ($\times 200$). (C) The growth of SW620 and HT29 cells was assessed by the colony formation assay. (D) Flow cytometry analysis of cell cycle progression. The quantified results of the cell cycle distribution are shown. (E) The apoptosis of CRC cells was detected by flow cytometry with an annexin V-APC/PI double staining kit. Three independent assays were performed in triplicate. The data are expressed as the mean \pm SD. * $P < .05$; ** $P < .01$; *** $P < .001$ versus the Vector + siControl group, # $P < .05$; ## $P < .01$; ### $P < .001$ versus the FOXF2 + siControl group.

13 postinjection, *in vivo* bioluminescent imaging was performed to monitor growth using an *in vivo* bioluminescence imaging system. The bioluminescence imaging analysis

revealed significantly less local invasion in the FOXF2 group than in the Vector group (Figure 5C; $P < .01$). IHC staining confirmed that the levels of FOXF2 and PRUNE2 were increased in

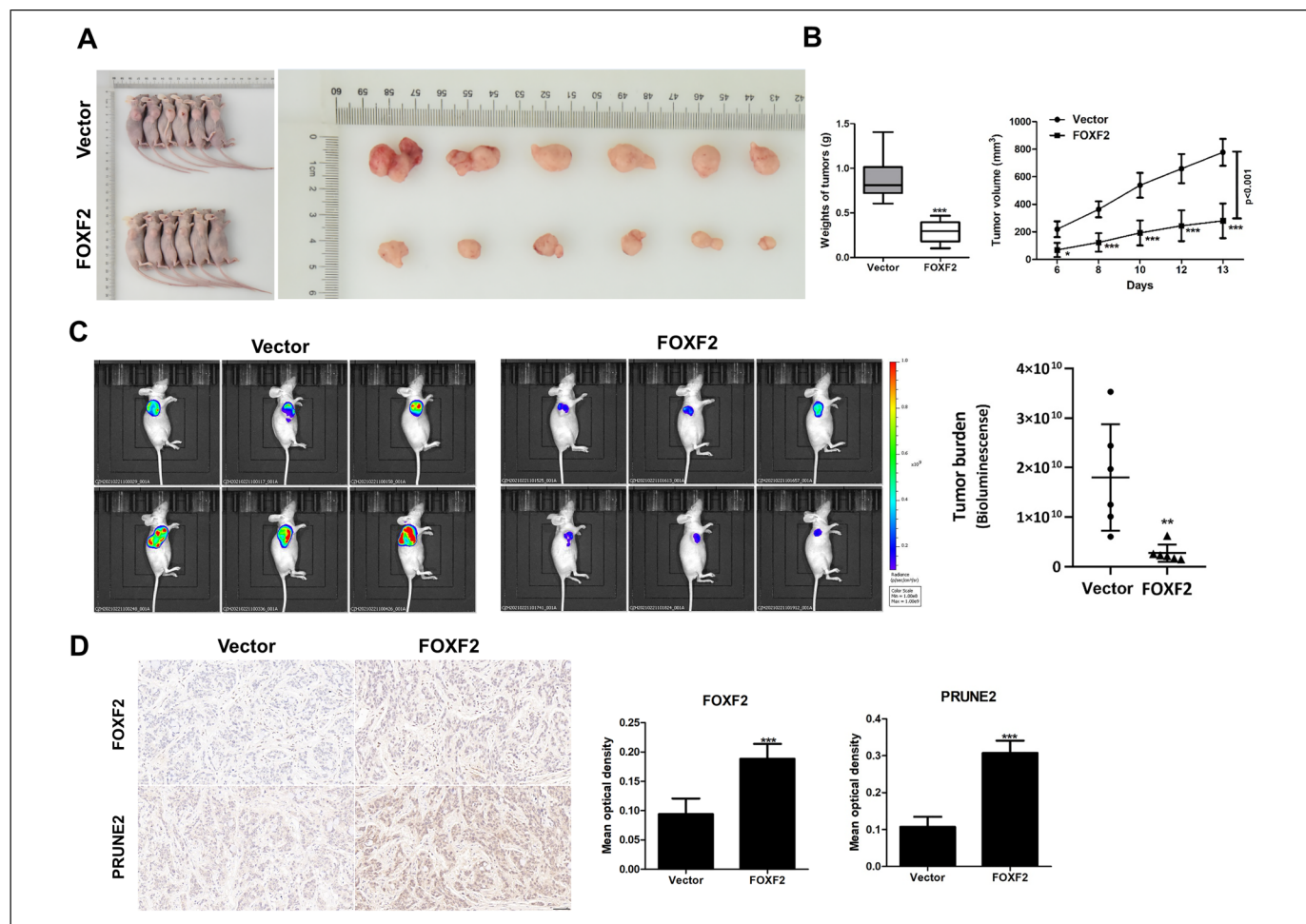


Figure 5. FOXF2 overexpression suppresses CRC cell growth *in vivo*. (A) Representative images of mice with xenograft tumors comprised of LV-GFP-FOXF2 cells or negative control cells on day 13 after the injection. (B) The weights of the xenograft tumors ($n = 6$) were measured on day 13 after the injection (left). The volumes of the xenograft tumors ($n = 6$) at the indicated time points are shown (right). (C) Bioluminescence images of the xenograft tumors of mice ($n = 6$) on day 13 after injection (left) and bioluminescence quantification of the whole body (right). (D) FOXF2 and PRUNE2 expression in xenograft tumor tissues were detected by immunohistochemistry ($\times 400$, left). Scale bar = 50 μm . Quantification of FOXF2 and PRUNE2 expression using ImageJ software (right). Three independent assays were performed in triplicate. The data are expressed as the mean \pm SD. * $P < .05$; ** $P < .01$; *** $P < .001$.

the xenograft tumors of mice overexpressing FOXF2 (Figure 5D, both $P < .001$).

Discussion

Therapies for CRC patients have been developed and evolved due to a better understanding of advances in the field of oncogenesis and genetics; however, even with these advances, there is still a lack of new biomarkers to guide early diagnosis, targeted therapy, prognosis, and monitoring of CRC patients. Therefore, we believe that the discovery and identification of novel genes with antiproliferative effects in CRC can provide potential molecular markers for the diagnosis, prediction, and prognosis of CRC.

The FOX transcription factor family, which contains a conserved DNA-binding domain with a winged helix structure, plays crucial roles in cell proliferation, apoptosis, the cell

cycle, signal transduction, and tumorigenesis.⁴⁶ Many FOX transcription factor subfamilies are importantly associated with the biological characteristics of CRC. FOXA1 expression was significantly increased in CRC, and its knockdown reduced proliferation, migration, and invasion and induced G2/M phase arrest in HCT116 and SW480 cells.⁴⁷ Gain-of-function assays of FOXF2 showed that high FOXF2 overexpression suppressed proliferation and invasion, and induced G0/G1 phase arrest and apoptosis in SW620 and HT29 cells, suggesting that FOXF2 helps to control the proliferation of CRC cells and inhibit their growth. FOXD3 is downregulated in CRC samples and can be regarded as a potential diagnostic biomarker in CRC.¹⁸ FOXK1 is highly expressed in CRC, and its overexpression promotes CRC cell malignancy by stimulating their proliferation and reducing their apoptosis.⁴⁸ FOXQ1 plays critical roles in the malignancy and progression of CRC.⁴⁹ Therefore, each FOX member plays a different role in the development of CRC.

Previous studies have demonstrated that the expression of FOXF2 is decreased in CRC and that its upregulation can inhibit CRC progression,^{18–20,22} indicating that FOXF2 dysregulation is also correlated with CRC development. In our study, FOXF2 expression was significantly decreased in CRC samples and cell lines, and FOXF2 overexpression reduced proliferation, migration, and invasion and induced G0/G1 phase arrest in SW620 and HT29 cells. Our results indicated that FOXF2 can be regarded as a potential diagnostic biomarker in CRC. FOXF2 was downregulated in CRC and can be regarded as a potential diagnostic biomarker in CRC.¹⁸ Our results are consistent with those of the abovementioned previous study. Together, these results indicate that FOXF2 promotes cell proliferation and plays a role in the pathogenesis and development of CRC. *In vivo*, FOXF2 overexpression significantly inhibited tumor growth in a xenograft tumor mouse assay. *In vitro*, FOXF2 overexpression inhibited the growth and invasion of CRC cells and promoted cell apoptosis. However, the mechanism by which FOXF2 regulates the development and progression of CRC remains unclear.

The FOX transcription factor family is encoded by the FOX gene, which mediates gene transcription and follow-up functions during physiological and pathological processes.⁵⁰ FOXF2 manipulates downstream pathways and targets as both a pro-oncogenic and anti-oncogenic factor across different types of cancer, suggesting that it can serve as a new clinical marker or therapeutic target for cancer. However, the biological functions and specific roles of FOXF2 in cancer development remain unclear. FOXF2, as a tumor suppressor, can inhibit the Wnt/ β -catenin pathway,^{26,51} the CDK2-RB-E2F cascade signaling pathway,⁵² and the VEGF-C/VEGFR3 signaling pathway⁵³ to reduce cell growth and induce apoptosis. However, other unknown regulatory signals may exist that are involved in the function of FOXF2. Analysis of data from TCGA revealed that FOXF2 expression was markedly decreased in CRC, indicating that low FOXF2 expression is involved in the aggressive behavior of CRC. Interestingly, we previously demonstrated that PRUNE2 has the same functions as FOXF2 in CRC, and the survival prognosis of patients with low expression of PRUNE2 was poor.⁴² Thus, we speculated that FOXF2 may regulate PRUNE2 and that this regulatory correlation may play an important role in CRC. Herein, we identified PRUNE2 as a novel transcriptional target of FOXF2 and demonstrated that FOXF2 regulated the proliferation and progression of CRC by positively regulating PRUNE2 transcription. From the dual-luciferase reporter assay, FOXF2 upregulation significantly enhanced the luciferase activity of pPRUNE2 #2 compared with that in the control cells and cells transfected with the other pPRUNE2 constructs (#1, #3, #4), suggesting that FOXF2 activates the PRUNE2 promoter by mainly binding to the S7-S14 regions. However, the luciferase activity induced by pPRUNE2 #1 (containing both S1-S6 and S7-S14 binding sites) was much lower than that induced by pPRUNE2 #2, indicating the potential existence of other regulators that can bind sites S1-S6 of the PRUNE2 promoter and thereby suppress its promoter activity, which needs to be further evaluated. These data demonstrate that PRUNE2 is a

downstream target of FOXF2 and that FOXF2 directly targets the PRUNE2 promoter and promotes its expression in CRC cells.

PRUNE2 is reported to regulate the differentiation, proliferation, and invasion of neuroblastoma tumor cells, and increased expression of PRUNE2 is associated with favorable prognosis in human patients with neuroblastomas.³⁶ A previous study demonstrated that PRUNE2 decreased cell survival, proliferation, invasion, and tumorigenicity and promoted apoptosis, suggesting that PRUNE2 functions as a tumor-suppressive gene in CRC.⁴² However, the role of PRUNE2 and its mechanism in CRC are still unclear. Taking the above into consideration, we assumed that PRUNE2 mediates the inhibitory function of FOXF2 in the development and pathogenesis of CRC. To prove the above hypothesis, we downregulated the expression of PRUNE2 in pcDNA3.1-FOXF2-transfected CRC cells. Downregulation of PRUNE2 rescued the decreased proliferation and invasion of CRC cells induced by FOXF2 overexpression. Moreover, downregulation of PRUNE2 inhibited CRC cell apoptosis and promoted cell cycle progression, which were accelerated and arrested by FOXF2 overexpression, respectively. IHC analysis of xenograft tumors showed that both FOXF2 and PRUNE2 were upregulated in the xenograft tumors of FOXF2-overexpressing mice compared with mice treated with the negative control vector. These results suggest that PRUNE2 mediates the FOXF2-regulated aggressive properties of CRC cells. However, downstream signaling pathways are activated by FOXF2 regulating PRUNE2 during the development of CRC remains unknown and requires further research.

Conclusion

In conclusion, we indicated that FOXF2 was involved in the pathogenesis of CRC *in vitro* and *in vivo*. PRUNE2, as a transcriptional target of FOXF2, at least partially mediates the functions of FOXF2 in CRC. Overexpression of FOXF2 suppresses the proliferation and invasion of CRC by positively regulating PRUNE2 expression. Moreover, the mRNA levels of FOXF2 and PRUNE2 are positively correlated with CRC. The FOXF2 mRNA level, particularly in combination with the PRUNE2 mRNA level, may serve as a prognostic marker for CRC patients. Based on these findings, we speculate that the FOXF2-PRUNE2 transcriptional regulation axis can serve as a candidate therapeutic target for aggressive CRC in future clinical research.

Authors' Note

The study was approved by the Ethics Committee of the First People's Hospital of Yunnan Province (no. KHLL2021-KY130). All the patients who enrolled in this research had signed the written informed consent voluntarily. Animal experiments were performed under a project license (no. GSZE0260446) granted by the Ethics Committee of Shanghai Genechem Co., Ltd, in compliance with Chinese national guidelines for the care and use of animals.

Declaration of Conflicting Interests

The author(s) declared no potential conflicts of interest with respect to the research, authorship, and/or publication of this article.

Funding

The author(s) disclosed receipt of the following financial support for the research, authorship, and/or publication of this article: This work was supported by the Joint Foundation of Kunming Medical University and Yunnan Provincial Science and Technology Department, Yunnan Health Training Project of High Level Talents, National Natural Science Foundation of China, the Clinical Medical Center of Yunnan Provincial Health Commission, Internal Division of Yunnan Provincial Health Commission (grant number 202001AY070001-114, 2019FE001-121, H-2018039, 81860522, 2020LCZXXF-XH03, 2018NS0263).

ORCID iD

Qiang Guo  <https://orcid.org/0000-0003-0636-5548>

References

- Bray F, Ferlay J, Soerjomataram I, Siegel RL, Torre LA, Jemal A. Global cancer statistics 2018: GLOBOCAN estimates of incidence and mortality worldwide for 36 cancers in 185 countries. *CA Cancer J Clin.* 2018;68(6):394-424.
- Arnold M, Sierra MS, Laversanne M, Soerjomataram I, Jemal A, Bray F. Global patterns and trends in colorectal cancer incidence and mortality. *Gut.* 2017;66(4):683-691.
- Weigel D, Jürgens G, Küttner F, Seifert E, Jäckle H. The homeotic gene fork head encodes a nuclear protein and is expressed in the terminal regions of the drosophila embryo. *Cell.* 1989;57(4):645-658.
- Jackson BC, Carpenter C, Nebert DW, Vasiliou V. Update of human and mouse forkhead box (FOX) gene families. *Hum Genomics.* 2010;4(5):345-352.
- Kaestner KH, Knochel W, Martinez DE. Unified nomenclature for the winged helix/forkhead transcription factors. *Genes Dev.* 2000;14(2):142-146.
- Carlsson P, Mahlapuu M. Forkhead transcription factors: key players in development and metabolism. *Dev Biol.* 2002;250(1):1-23.
- Benayoun BA, Caburet S, Veitia RA. Forkhead transcription factors: key players in health and disease. *Trends Genet.* 2011;27(6):224-232.
- Ormestad M, Astorga J, Landgren H, et al. Foxf1 and Foxf2 control murine gut development by limiting mesenchymal Wnt signaling and promoting extracellular matrix production. *Development.* 2006;133(5):833-843.
- Aitola M, Carlsson P, Mahlapuu M, Enerbäck S, Pelto-Huikko M. Forkhead transcription factor FoxF2 is expressed in mesodermal tissues involved in epithelio-mesenchymal interactions. *Dev Dyn.* 2000;218(1):136-149.
- Wang T, Tamakoshi T, Uezato T, et al. Forkhead transcription factor Foxf2 (LUN)-deficient mice exhibit abnormal development of secondary palate. *Dev Biol.* 2003;259(1):83-94.
- Zhang T, Wan JG, Liu JB, Deng M. MiR-200c inhibits metastasis of breast tumor via the downregulation of Foxf2. *Genet Mol Res.* 2017;16(3).
- Cai J, Tian AX, Wang QS, et al. FOXF2 Suppresses the FOXC2-mediated epithelial-mesenchymal transition and multi-drug resistance of basal-like breast cancer. *Cancer Lett.* 2015;367(2):129-137.
- Kong PZ, Li GM, Tian Y, Song B, Shi R. Decreased expression of FOXF2 as new predictor of poor prognosis in stage I non-small cell lung cancer. *Oncotarget.* 2016;7(34):55601-55610.
- Kundu ST, Byers LA, Peng DH, et al. The miR-200 family and the miR-183~96~182 cluster target Foxf2 to inhibit invasion and metastasis in lung cancers. *Oncogene.* 2016;35(2):173-186.
- Xu JL, Hua T, Ding J, Fan Y, Liu ZJ, Lian JW. FOXF2 Aggravates the progression of non-small cell lung cancer through targeting lncRNA H19 to downregulate PTEN. *Eur Rev Med Pharmacol Sci.* 2019;23(24):10796-10802.
- Dou C, Jin X, Sun L, Zhang B, Han M, Li T. FOXF2 Deficiency promotes hepatocellular carcinoma metastasis by inducing mesenchymal-epithelial transition. *Cancer Biomark.* 2017;19(4):447-454.
- Shi Z, Liu J, Yu X, et al. Loss of FOXF2 expression predicts poor prognosis in hepatocellular carcinoma patients. *Ann Surg Oncol.* 2016;23(1):211-217.
- Hauptman N, Jevšinek Skok D, Spasovska E, Boštjančič E, Glavač D. Genes CEP55, FOXD3, FOXF2, GNAO1, GRIA4, and KCNA5 as potential diagnostic biomarkers in colorectal cancer. *BMC Med Genet.* 2019;12(1):54.
- Zhang Y, Wang X, Wang Z, Tang H, Fan H, Guo Q. miR-182 promotes cell growth and invasion by targeting forkhead box F2 transcription factor in colorectal cancer. *Oncol Rep.* 2015;33(5):2592-2598.
- Chen W, Tong K, Yu J. MicroRNA-130a is upregulated in colorectal cancer and promotes cell growth and motility by directly targeting forkhead box F2. *Mol Med Rep.* 2017;16(4):5241-5248.
- Chen J, Ding J, Wang Z, Zhu J, Wang X, Du J. Identification of downstream metastasis-associated target genes regulated by LSD1 in colon cancer cells. *Oncotarget.* 2017;8(12):19609-19630.
- Dai W, Zeng W, Lee D. lncRNA MCM3AP-AS1 inhibits the progression of colorectal cancer via the miR-19a-3p/FOXF2 axis. *J Gene Med.* 2021;23(3):e3306.
- van der Heul-Nieuwenhuijsen L, Dits NF, Jenster G. Gene expression of forkhead transcription factors in the normal and diseased human prostate. *BJU Int.* 2009;103(11):1574-1580.
- van der Heul-Nieuwenhuijsen L, Dits N, Van Ijcken W, de Lange D, Jenster G. The FOXF2 pathway in the human prostate stroma. *Prostate.* 2009;69(14):1538-1547.
- Wei WR, Zeng GJ, Liu C, Zou BW, Li L. Overexpression of miR-96 promotes cell proliferation by targeting FOXF2 in prostate cancer. *Int J Clin Exp Pathol.* 2017;10(7):7596-7602.
- Higashimori A, Dong Y, Zhang Y, et al. Forkhead Box F2 suppresses gastric cancer through a novel FOXF2-IRF2BPL- β -catenin signaling axis. *Cancer Res.* 2018;78(7):1643-1656.
- Zhang C, Li Y, Dai D. Aberrant DNA methylation-mediated FOXF2 dysregulation is a prognostic risk factor for gastric cancer. *Front Mol Biosci.* 2021;8:645470.
- Wang H, Ma N, Li W, Wang Z. MicroRNA-96-5p promotes proliferation, invasion and EMT of oral carcinoma cells by directly targeting FOXF2. *Biol Open.* 2020;9(3).
- Wang A, Jin C, Li H, Qin Q, Li L. lncRNA ADAMTS9-AS2 regulates ovarian cancer progression by targeting miR-182-5p/FOXF2 signaling pathway. *Int J Biol Macromol.* 2018;120(Pt B):1705-1713.

30. Milewski D, Pradhan A, Wang X, et al. Foxf1 and FoxF2 transcription factors synergistically promote rhabdomyosarcoma carcinogenesis by repressing transcription of p21 CDK inhibitor. *Oncogene*. 2017;36(6):850-862.
31. Zhang Z, Wang C, Liu T, et al. miRNA-182-5p promotes human bladder cancer proliferation and migration through the FOXF2/SHH axis. *Neoplasma*. 2022;69(2): 321-330.
32. Chen X, Hu H, Liu J, et al. FOXF2 promoter methylation is associated with prognosis in esophageal squamous cell carcinoma. *Tumour Biol*. 2017;39(2):1010428317692230.
33. Wang S, Li GX, Tan CC, et al. FOXF2 Reprograms breast cancer cells into bone metastasis seeds. *Nat Commun*. 2019;10(1):2707.
34. Lu JT, Tan CC, Wu XR, et al. FOXF2 Deficiency accelerates the visceral metastasis of basal-like breast cancer by unrestrictedly increasing TGF- β and miR-182-5p. *Cell Death Differ*. 2020;27(10):2973-2987.
35. Pan CQ, Low BC. Functional plasticity of the BNIP-2 and Cdc42GAP Homology (BCH) domain in cell signaling and cell dynamics. *FEBS Lett*. 2012;586(17):2674-2691.
36. Machida T, Fujita T, Ooo ML, et al. Increased expression of pro-apoptotic BMCC1, a novel gene with the BNIP2 and Cdc42GAP homology (BCH) domain, is associated with favorable prognosis in human neuroblastomas. *Oncogene*. 2006;25(13):1931-1942.
37. Zhao LR, Tian W, Wang GW, Chen KX, Yang JL. The prognostic role of PRUNE2 in leiomyosarcoma. *Chin J Cancer*. 2013;32(12):648-652.
38. Su SC, Yeh CM, Lin CW, et al. A novel melatonin-regulated lncRNA suppresses TPA-induced oral cancer cell motility through replenishing PRUNE2 expression. *J Pineal Res*. 2021;71(3):e12760.
39. Drayton RM, Rehman I, Clarke R, et al. Identification and diagnostic performance of a small RNA within the PCA3 and BMCC1 gene locus that potentially targets mRNA. *Cancer Epidemiol Biomarkers Prev*. 2015;24(1):268-275.
40. Harris JL, Richards RS, Chow CW, et al. BMCC1 Is an AP-2 associated endosomal protein in prostate cancer cells. *PLoS One*. 2013;8(9):e73880.
41. Islam MS, Takano R, Yokochi T, et al. Programmed expression of pro-apoptotic BMCC1 during apoptosis, triggered by DNA damage in neuroblastoma cells. *BMC Cancer*. 2019;19(1):542.
42. Li T, Huang S, Yan W, Zhang Y, Guo Q. PRUNE2 inhibits progression of colorectal cancer in vitro and in vivo. *Exp Ther Med*. 2022;23(2):169.
43. Comprehensive molecular characterization of human colon and rectal cancer. *Nature*. 2012;487(7407):330-337.
44. Zhou N, Yan B, Ma J, et al. Expression of TCF3 in Wilms' tumor and its regulatory role in kidney tumor cell viability, migration and apoptosis in vitro. *Mol Med Rep*. 2021;24(3).
45. Livak KJ, Schmittgen TD. Analysis of relative gene expression data using real-time quantitative PCR and the 2^{(-Delta Delta C(T))} method. *Methods*. 2001;25(4):402-408.
46. Katoh M, Katoh M. Human FOX gene family (Review). *Int J Oncol*. 2004;25(5):1495-1500.
47. Pan J, Xu Z, Xu M, Lin X, Lin B, Lin M. Knockdown of forkhead box A1 suppresses the tumorigenesis and progression of human colon cancer cells through regulating the phosphatase and tensin homolog/Akt pathway. *J Int Med Res*. 2020;48(12):300060520971453.
48. Wu W, Chen Y, Ye S, Yang H, Yang J, Quan J. Transcription factor forkhead box K1 regulates miR-32 expression and enhances cell proliferation in colorectal cancer. *Oncol Lett*. 2021;21(5):407.
49. Tang H, Zheng J, Bai X, et al. Forkhead box Q1 is critical to angiogenesis and macrophage recruitment of colorectal cancer. *Front Oncol*. 2020;10:564298.
50. Wu Q, Li W, You C. The regulatory roles and mechanisms of the transcription factor FOXF2 in human diseases. *PeerJ*. 2021;9:e10845.
51. Nik AM, Reyahi A, Ponten F, Carlsson P. Foxf2 in intestinal fibroblasts reduces numbers of Lgr5(+) stem cells and adenoma formation by inhibiting Wnt signaling. *Gastroenterology*. 2013;144(5):1001-1011.
52. Lo PK, Lee JS, Liang X, Sukumar S. The dual role of FOXF2 in regulation of DNA replication and the epithelial-mesenchymal transition in breast cancer progression. *Cell Signal*. 2016;28(10):1502-1519.
53. Wang QS, He R, Yang F, et al. FOXF2 Deficiency permits basal-like breast cancer cells to form lymphangiogenic mimicry by enhancing the response of VEGF-C/VEGFR3 signaling pathway. *Cancer Lett*. 2018;420:116-126.